

# Excitation of $S_{11}$ resonances in pion scattering and pion photoproduction on the proton

Guan-Yeu Chen, Sabit Kamalov\* and Shin Nan Yang

*Department of Physics, National Taiwan University, Taipei, Taiwan 10764, Republic of China*

Dieter Drechsel and Lothar Tiator

*Institut für Kernphysik, Universität Mainz, 55099 Mainz, Germany*

(October 29, 2018)

A self-consistent analysis of pion scattering and pion photoproduction within a coupled channels dynamical model is presented. In the case of pion photoproduction, we obtain background contributions to the imaginary part of the  $S$ -wave multipole which differ considerably from the result based on the K-matrix approximation. Within the dynamical model these background contributions become large and negative in the region of the  $S_{11}(1535)$  resonance. Due to this fact much larger resonance contributions are required in order to explain the results of the recent multipole analyses. For the first  $S_{11}(1535)$  resonance we obtain as a value of the dressed electromagnetic helicity amplitude:  $A_{1/2} = (72 \pm 2) \times 10^{-3} \text{GeV}^{-1/2}$ . Similar values can be derived from eta photoproduction if one takes the same total width ( $\Gamma_R = 95 \pm 5 \text{ MeV}$ ) as in pion scattering and pion photoproduction. The combined analysis yields considerable strength at invariant mass  $W \geq 1750 \text{ MeV}$ , which can be explained by a third and a fourth  $S_{11}$  resonance with the masses  $1846 \pm 47$  and  $2113 \pm 70 \text{ MeV}$ .

PACS numbers: 13.60.Le, 13.75.Gx, 14.20.Gk, 25.20.Lj

## I. INTRODUCTION

Hadron spectroscopy has always played an important role in unraveling the underlying quark dynamics. For example, the pattern of similarity between the eight baryons and the eight pseudoscalar mesons led to the epochal discovery of SU(3) symmetry.

There are 44 nonstrange baryon states listed in the Particle Data Group [1], 22 in  $T = \frac{1}{2}$  and another 22 in  $T = \frac{3}{2}$  channels. Among them, 18 are rated four-star and 6 rated three-star. The rest are weakly excited states with at most fair evidence of existence. Even though the existence of the four-star baryon resonances is certain, some very large discrepancies exist in their properties as obtained from different analyses. One example is the extracted width of the four-star  $S_{11}(1535)$  state given as 66 MeV [2],  $120 \pm 20 \text{ MeV}$  [3],  $151 \pm 27 \text{ MeV}$  [4],  $151 - 198 \text{ MeV}$  [5], and  $270 \pm 50 \text{ MeV}$  [6]. The differences between different analyses arise mostly from the data set included in the analysis or the separation of background and resonance contributions. This model dependence in the extraction of the resonance properties has made it difficult to test the predictions of theoretical models with existing data.

At present the resonance properties are extracted mainly from  $\pi N$  scattering,  $2\pi$  and  $\eta$  production and pion photoproduction using different approaches (for details see Refs. [7–10]). The first coupled channel analysis that combines pion and eta data was done in Ref. [7] within the isobar model. Later, more sophisticated models were developed which account for background contributions. Most of them are based on the solution of coupled-channels equations by use of the K-matrix approximation, i.e., by ignoring off-shell intermediate scattering states. A motivation for such an approximation is the result of Ref. [11], where it was shown that off-shell effects could be incorporated into the vertex renormalization of the lowest order Lagrangians.

On the other hand, in the analysis of pion scattering and pion photoproduction within dynamical models [12–14], the off-shell dynamics (i.e., the dynamics at short distance) is taken into account. Within this framework we have recently developed a meson-exchange (MEX) model for pion-nucleon scattering [15] which gives good agreement with the data up to 400 MeV pion lab energy. In addition, we have also constructed a dynamical model for pion electromagnetic production [16,17] which describes the  $\pi^0$  photo- and electro-production data near threshold [18] and most of the existing data up to the second resonance region.

In this paper, we extend our meson-exchange  $\pi N$  model in the  $S_{11}$  channel up to 2 GeV by explicitly introducing a set of  $S_{11}$  resonances into the model. The results are then fed into the pion photoproduction model to analyze the existing  ${}_p E_{0+}$  multipole. The  $S_{11}$  channel is of interest for several reasons. First of all, the first resonance  $S_{11}(1535)$ , which lies only 48 MeV above the  $\eta N$  threshold, has a remarkably large  $\eta N$  branching ratio. This necessitates the inclusion of the  $\eta N$  channel into our MEX  $\pi N$  model. Secondly, the analyses based solely on pion photoproduction always underestimate the  $A_{1/2}^p$  helicity amplitude of  $S_{11}(1535)$  with a value around  $60 \times 10^{-3} \text{GeV}^{-1/2}$ , while extractions

from the  $(\gamma, \eta)$  data give a value close to and above  $100 \times 10^{-3} \text{GeV}^{-1/2}$  [1]. Lastly, there have been suggestions [19,20] that there could exist a third  $S_{11}$  resonance in the neighborhood of 1800 – 1900 MeV, in addition to the well-known resonances at 1535 and 1650 MeV. A consistent analysis of both  $\pi N$  scattering and pion photoproduction reactions can shed new light on the mentioned issues concerning helicity amplitudes and higher resonance as well as reduce the large uncertainties in the width obtained from previous analyses.

## II. $\pi N$ SCATTERING

Our MEX  $\pi N$  model results by use of a three-dimensional reduction scheme of the Bethe-Salpeter equation for a model Lagrangian involving  $\pi, N, \Delta, \rho,$  and  $\sigma$  fields. Details can be found in Ref. [15]. Here we only present the general scheme to extend the model to the case of coupled  $\pi, \eta,$  and  $2\pi$  channels, including in addition the couplings with baryon resonances in the  $S_{11}$  partial wave. To do this, we first enlarge the Hilbert space to include a bare  $S_{11}$  particle  $R$  which acquires a width by couplings with  $\pi N$  and  $\eta N$  channels via the Lagrangian

$$\mathcal{L}_{\mathcal{I}} = ig_{\pi NR}^{(0)} \bar{R} \boldsymbol{\tau} N \cdot \boldsymbol{\pi} + ig_{\eta NR}^{(0)} \bar{R} N \eta + h.c., \quad (1)$$

where  $N, R, \boldsymbol{\pi},$  and  $\eta$  denote the field operators for the nucleon, bare  $R$ , pion and eta, respectively. The full  $t$ -matrix can then be written as a system of coupled equations,

$$t_{ij}(E) = v_{ij}(E) + \sum_k v_{ik}(E) g_k(E) t_{kj}(E), \quad (2)$$

where  $i$  and  $j$  denote the  $\pi$  or  $\eta$  channel and  $E = W$  is the total center of mass energy. Equation (2) is a system of three-dimensional coupled integral equations which is derived from the four-dimensional Bethe-Salpeter equation using a three-dimensional reduction scheme with a relativistic propagator  $g_k$  for the free  $kN$  system ( $k = \pi,$  or  $\eta$ ), constructed according to the Cooper-Jennings reduction scheme [21].

In general, the potential  $v_{ij}$  is a sum of non-resonant ( $v_{ij}^B$ ) and bare resonance ( $v_{ij}^R$ ) terms,

$$v_{ij}(E) = v_{ij}^B(E) + v_{ij}^R(E). \quad (3)$$

The non-resonant term  $v_{\pi\pi}^B$  for the  $\pi N$  elastic channels contains contributions from the  $s$ - and  $u$ -channels, Born terms and  $t$ -channel contributions with  $\omega, \rho,$  and  $\sigma$  exchange. In the present work the parameters in  $v_{\pi\pi}^B$  are fixed from the analysis of the pion scattering phase shifts for the  $s$ - and  $p$ -waves at low energies ( $W < 1300$  MeV). In channels involving the eta,  $v_{i\eta}^B$  is taken to be zero because of the small  $\eta NN$  coupling [22]. The bare resonance contribution  $v_{ij}^R(E)$  arises from excitation and de-excitation of the resonance  $R$  via the interaction Lagrangian of Eq. (1).

Let us first consider the case with only one  $S_{11}$  resonance contributing in the energy region of interest, i.e.,  $W < 2$  GeV. The corresponding potential  $v_{ij}^R(E)$  can then be symbolically expressed in the form of

$$v_{ij}^R(q, q'; E) = \frac{f_i(\tilde{\Lambda}_i, q; E) g_i^{(0)} g_j^{(0)} f_j(\tilde{\Lambda}_j, q'; E)}{E - M_R^{(0)} + i\frac{1}{2}\Gamma_{2\pi}^R(E)}, \quad (4)$$

where  $q$  and  $q'$  are the pion (or eta) momenta in the initial and final states, and  $M_R^{(0)}$  and  $g_{i(j)}^{(0)}$  are the bare masses and resonance vertex couplings, respectively. According to our previous  $\pi N$  model, we associate with each line of the particle  $\alpha$  in a Feynman diagram the covariant form factor  $F_\alpha [n_\alpha \Lambda_\alpha^4 / (n_\alpha \Lambda_\alpha^4 + (p_\alpha^2 - m_\alpha^2)^2)]^{n_\alpha}$ , where  $p_\alpha, m_\alpha,$  and  $\Lambda_\alpha$  are the four-momentum, mass, and cut-off parameter of particle  $\alpha$ , respectively. The quantity  $f_i$  of Eq. (4) is then a product of three form factors  $F_\alpha$ , each of them corresponding to one of the three legs associated with the considered vertex. As a result,  $f_i$  depends on the product of three cut-off parameters, i.e.,  $\tilde{\Lambda}_\pi \equiv (\Lambda_N, \Lambda_R, \Lambda_\pi)$ . We refer the readers to Refs. [15,23] for details and only mention that  $n_\alpha = 10$  is used in the present work.

In Eq. (4) we have added a phenomenological term  $\Gamma_{2\pi}^R(E)$  in the resonance propagator in order to take into account the  $\pi\pi N$  decay channel. Therefore, our resonance propagator is not purely "bare" but includes renormalization (or "dressing") effects due to the coupling with the  $\pi\pi N$  channel. Using this prescription we assume that the additional non-resonant mechanisms of coupling with the  $\pi\pi N$  channel are small. Following Refs. [24,25] we take  $\Gamma_{2\pi}^R(E)$  as

$$\Gamma_{2\pi}^R(E) = \Gamma_{2\pi}^{0,R} \left( \frac{q_{2\pi}}{q_0} \right)^{2l+4} \left( \frac{X^2 + q_0^2}{X^2 + q_{2\pi}^2} \right)^{l+2}, \quad (5)$$

where  $l$  is the pion orbital momentum,  $q_{2\pi}$  the momentum of the compound  $2\pi$  system with mass  $2m_\pi$  and  $q_0 = q_{2\pi}$  at  $E = M_R^{(0)}$ . We note that this form takes account of the correct energy behavior of the phase space near the three-body threshold [24]. The parameter  $X$  is fixed at 500 MeV as suggested in Ref. [25], and the quantity  $\Gamma_{2\pi}^{0,R}$  is associated with the  $2\pi$  decay width at resonance. In general,  $\Gamma_{2\pi}^{0,R}$  can be considered as a free parameter. However, its value is strongly correlated with the values of the unknown coupling constants  $g_i^{(0)}$ . In particular, a small  $g_i^{(0)}$  usually requires a large  $\Gamma_{2\pi}^{0,R}$ . Therefore, we will fix the value for  $\Gamma_{2\pi}^{0,R}$  by use of recent knowledge about the decay modes of the resonances and their total Breit-Wigner widths [1].

Summarizing our parametrization of the potential  $v_{ij}^R$  in the case of coupled pion and eta channels, we would like to emphasize that, in general, one isolated resonance contains five free parameters, the bare mass  $M_R^{(0)}$ , the decay width  $\Gamma_{2\pi}^0$ , two bare coupling constants  $g_i^{(0)}$  and  $g_j^{(0)}$ , and one cutoff parameter  $\Lambda_R$ .

In the channel of interest,  $S_{11}$ , there are two well-known four-star resonance states,  $S_{11}(1535)$  and  $S_{11}(1650)$ , and one one-star resonance,  $S_{11}(2090)$ . In the Hypercentral Constituent Quark Model [19], a third and fourth  $S_{11}$  resonance with energies 1860 and 2008 MeV were predicted. The generalization of our coupled channels model for multiple resonances with the same quantum numbers is simply

$$v_{ij}^R(q, q'; E) = \sum_{n=1}^N v_{ij}^{R_n}(q, q'; E), \quad (6)$$

with additional parameters for the bare masses, widths, coupling constants and cut-off parameters for each resonance.

We first start with the analysis of  $\text{Re } t_{ij}$  and  $\text{Im } t_{ij}$  for pion scattering and eta production in the energy range  $1100 \text{ MeV} < W < 1750 \text{ MeV}$  where the  $S_{11}(1535)$  and  $S_{11}(1650)$  resonances are very pronounced. The results of our best fit of  $t_{\pi\pi}$  in this energy range with only these two resonances included are shown in Fig. 1 by the dotted curves. We are not able to improve our results in the region  $W > 1800 \text{ MeV}$  without additional  $S_{11}$  resonances. Next we extend the energy range up to  $W = 2000 \text{ MeV}$  and add a third resonance with the parameters for the first resonance fixed as obtained above. Our results for this case are shown by the dash-dotted curves, which correspond to a bare mass of the third  $S_{11}$  resonance  $M_3^{(0)} = 1901 \text{ MeV}$ . We find that this value is very stable and changes only within 2% if the energy range is increased up to 2200 MeV. However, this does not remove the remaining discrepancy, in particular for the imaginary part at  $W > 2000 \text{ MeV}$ . We find that the only way to improve the agreement with the data in this energy range is to introduce a fourth resonance. Our final fit results ( $\chi^2/120 = 4.56$ ) with four  $S_{11}$  resonances are shown by the solid lines in Fig. 1. The obtained value for the bare mass of the fourth  $S_{11}$  resonance is  $M_4^{(0)} = 2160 \text{ MeV}$ . Note that in Fig. 1 the background contributions (dashed curves) are defined by the equation

$$\tilde{t}_{\pi\pi}^B(E) = v_{\pi\pi}^B(E) + v_{\pi\pi}^B(E) g(E) \tilde{t}_{\pi\pi}^B(E), \quad (7)$$

which are hereafter called the "nonresonant background", i.e., the background with nonresonant rescattering. In the following Fig. 2 we show our results for the  $t$ -matrix of the  $\pi N \rightarrow \eta N$  reaction in the  $S_{11}$  channel, which clearly indicate the presence of the  $\eta$  decay mode in the second and third  $S_{11}$  resonance regions.

Now let us turn to the more sophisticated part of the analysis, namely, the extraction of the physical (or "dressed") masses, partial widths and branching ratios of the resonances. As was pointed out in Ref. [9], the procedure is certainly model dependent. This is mainly connected with the question how to separate background and resonance contributions in a well-defined way. The solution to this problem becomes more difficult with an increasing number of overlapping resonances in the same channel. Below we present our solution to this problem.

First, we determine the physical mass using as definition for the contribution of the  $n$ -th resonance  $R_n$  in the elastic pion scattering channel:

$$t_{\pi\pi}^{R_n}(E) = v_{\pi\pi}^{R_n}(E) + \sum_k v_{\pi k}^{R_n}(E) g_k(E) t_{k\pi}(E), \quad (8)$$

with  $t_{k\pi}(E)$  the full  $t$ -matrix obtained from the solution of Eq. (2). It is easy to see that Eq. (8) corresponds to the following decomposition of the full  $t_{\pi\pi}$  matrix:

$$t_{\pi\pi}(E) = t_{\pi\pi}^B(E) + \sum_{n=1}^N t_{\pi\pi}^{R_n}(E), \quad (9)$$

where the new background operator is defined as

$$t_{\pi\pi}^B(E) = v_{\pi\pi}^B(E) + \sum_k v_{\pi k}^B(E) g_k(E) t_{k\pi}(E). \quad (10)$$

We call this the "resonant background", because it contains resonance contributions via the full scattering matrix  $t_{k\pi}(E)$ .

It can be shown that the sum of the two terms on the r.h.s. of Eq. (8) can be expressed by a single term as represented by the diagram on the l.h.s. in Fig. 3, which consists of a bare initial  $\pi NR_n$  vertex, followed by a dressed resonance propagator and then finally decay through a dressed  $\pi NR_n$  vertex. It now becomes obvious that  $t_{\pi\pi}^{R_n}$  should have the standard Breit-Wigner form,  $\sim (W - M_{R_n} + i\Gamma_{R_n}/2)^{-1}$ , near the resonance position. The energy  $W$  where  $\text{Re } t_{\pi\pi}^{R_n}$  crosses zero can be considered as the physical mass of the resonance  $R_n$ . The total width can be determined by the full width at half maximum of  $\text{Im } t_{\pi\pi}^{R_n}(W)$ . The branching ratios for the pion, eta and two-pion decay modes can be extracted from the corresponding self-energies calculated by projection of the  $t_{\pi\pi}^{R_n}$ -matrix on the standard Breit-Wigner form.

Our final results for the resonance parameters are summarized in Table I. Here we also compare with the results of the GW-Giessen collaboration, Pitt-ANL collaboration and Kent State University (KSU) group, taken from Ref. [10]. Our parameters for the first and second  $S_{11}$  resonances are close to the Pitt-ANL results. Both models predict a total width  $\Gamma_{R_1} \simeq 100$  MeV for the first and  $\Gamma_{R_2} \simeq 200$  MeV for the second  $S_{11}$  resonance. Note that the value obtained for the total width of the  $S_{11}(1535)$  is very close to the recent result of Ref. [27] (94 MeV) and Ref. [28] (106 MeV). However, there is no agreement with the results of the GW-Giessen model, which yields  $\Gamma_{R_1} \simeq 230$  MeV, and the KSU model, which yields  $\Gamma_{R_2} \simeq 108$  MeV. In the last case the reason for the discrepancy could be the absence of the  $\eta N$  production data in the fit of that reference. Within our model we can get a similar result for  $\Gamma_{R_2}$  if we also exclude this channel from our data base. Further differences lie in the parameters for the third  $S_{11}$ . The position and total width of this resonance in our and the Pitt-ANL analyses are close, but our model suggests a strong one-pion decay mode (about 40%), while the Pitt-ANL value is only 17%. The situation with the strength of the eta decay mode is opposite: we find a branching ratio of 12% as opposed to 41% in the Pitt-ANL analysis. As we will see below such differences have visible consequences for the pion and eta photoproduction. We further note that in the case of the third  $S_{11}$ , results similar to ours were also obtained in Ref. [8] ( $\Gamma_\pi/\Gamma_R = 51\%$ ).

### III. PION PHOTOPRODUCTION

The above analysis of elastic  $\pi N$  scattering indicates the existence of four  $S_{11}$  resonances. Let us now check this result by an independent analysis of pion photoproduction using the dynamical model developed in Refs. [13,16,17], hereafter called the DMT (Dubna-Mainz-Taipei) model. Concerning the details of the DMT model, we refer the reader to Ref. [16].

The t-matrix for pion photoproduction in the dynamical model is

$$t_{\gamma\pi}(E) = v_{\gamma\pi} + \sum_k v_{\gamma k} g_k(E) t_{k\pi}(E), \quad (11)$$

with  $v_{\gamma k}$  the transition potential for the  $\gamma N \rightarrow kN$  reaction ( $k = \pi$  or  $\eta$ ),  $t_{k\pi}$  the full  $kN$  scattering t-matrix of Eq. (2), and  $g_k$  the free  $kN$  propagator.

If the transition potential  $v_{\gamma\pi}$  consists of two terms,

$$v_{\gamma\pi}(E) = v_{\gamma\pi}^B + v_{\gamma\pi}^R(E), \quad (12)$$

where  $v_{\gamma\pi}^B$  is the background transition potential and  $v_{\gamma\pi}^R(E)$  the contribution of a bare resonance R, we may decompose the resulting t-matrix into two terms [16],

$$t_{\gamma\pi}(E) = t_{\gamma\pi}^B(E) + t_{\gamma\pi}^R(E), \quad (13)$$

where

$$t_{\gamma\pi}^B(E) = v_{\gamma\pi}^B + \sum_k v_{\gamma k}^B g_k(E) t_{k\pi}(E), \quad (14)$$

$$t_{\gamma\pi}^R(E) = v_{\gamma\pi}^R + \sum_k v_{\gamma k}^R g_k(E) t_{k\pi}(E). \quad (15)$$

In our numerical calculations we have neglected the contribution of the  $\eta$  channel in the intermediate states in Eq. (14), because this contribution is found to be much smaller than for the  $\pi$  channels. We further note that all the

processes which start with the excitation of the resonance by the bare  $\gamma NR$  vertex are summed up in  $t_{\gamma\pi}^R$ . This is similar to our definition Eq. (8) of the resonance contribution for  $\pi N$  scattering. Using the decomposition of Eqs. (13-15) we can now extract the value of the bare  $\gamma NR$  vertex. As in the case of pion scattering (see Eq. (10)), the corresponding background  $t_{\gamma\pi}^B$  is called "resonant background" since it contains the full pion scattering  $t$ -matrix. Note that, for example, in Ref. [29] the background is defined differently,

$$\tilde{t}_{\gamma\pi}^B(E) = v_{\gamma\pi}^B + v_{\gamma\pi}^B g_\pi(E) \tilde{t}_{\pi\pi}^B(E), \quad (16)$$

where  $\tilde{t}_{\pi\pi}^B$  is defined by Eq. (7). This definition corresponds to the so-called nonresonant (smooth) background, because it contains none of the resonance contributions. The corresponding resonance term  $\tilde{t}_{\gamma\pi}^R = t_{\gamma\pi} - \tilde{t}_{\gamma\pi}^B$  describes a resonance with a dressed  $\gamma NR$  vertex.

It can be easily proved that the following relation holds between  $t_{\gamma\pi}^R$  and  $\tilde{t}_{\gamma\pi}^R$ :

$$\tilde{t}_{\gamma\pi}^R(E) = t_{\gamma\pi}^R(E) + v_{\gamma\pi}^B g_\pi(E) \tilde{t}_{\pi\pi}^R(E), \quad (17)$$

where  $\tilde{t}_{\pi\pi}^R(E) = t_{\pi\pi}(E) - \tilde{t}_{\pi\pi}^B(E)$  is the dressed resonance contribution in pion scattering, as is graphically illustrated in Fig. 4.

The background potential  $v_{\gamma\pi}^B$  contains Born terms with an energy dependent mixing of pseudovector and pseudoscalar  $\pi NN$  coupling and  $t$ -channel vector meson exchanges [25]. The mixing parameters and coupling constants were determined from an analysis of the nonresonant multipoles. The standard physical multipoles in a channel  $\alpha = \{l, j, I\}$  can then be expressed as

$$t_{\gamma\pi}^{B,\alpha}(q_E, k) = v_{\gamma\pi}^{B,\alpha}(q_E, k) [1 + iq_E F_{\pi\pi}^{(\alpha)}(q_E, q_E; E)] - \frac{P}{\pi} \int_0^\infty \frac{q'^2 dq'}{\mathcal{M}(q')} \frac{F_{\pi\pi}^{(\alpha)}(q_E, q'; E) v_{\gamma\pi}^{B,\alpha}(q', k)}{E - E_{\pi N}(q')}, \quad (18)$$

where  $F_{\pi\pi}^{(\alpha)}$  is the pion-scattering amplitude with the on-shell value  $F_{\pi\pi}^{(\alpha)}(q_E, q_E) = [\eta_\alpha \exp(2i\delta_\alpha) - 1]/2iq_E$ , with  $\delta_\alpha$  the phase shift and  $\eta_\alpha$  the inelasticity parameter, and  $\mathcal{M}(q) = E_\pi(q)E_N(q)/E_{\pi N}(q)$  the relativistic pion-nucleon reduced mass. We mention in passing that the so-called "K-matrix" approximation, as in the case of MAID [25,30] and many others models, neglects the principal value integral in Eq. (18), and parametrizes the background in terms of on-shell pion rescattering only. In this case, the off-shell rescattering associated with the principal value integral contribution is phenomenologically absorbed in the resonance parameters, while in the DMT model it is considered as a part of the background. Therefore, the resonance parts in DMT and K-matrix approach are different: in the DMT model the resonance is described by the amplitude  $t_{\gamma\pi}^R$  with a bare electromagnetic vertex and, as we will see below, in the models based on the K-matrix approximation, the resonance description is essentially given by  $\tilde{t}_{\gamma\pi}^R$  with a dressed electromagnetic vertex.

Following Ref. [25], we assume a Breit-Wigner form for the resonance contribution  $t_{\gamma\pi}^{R,\alpha}(W)$ ,

$$t_{\gamma\pi}^{R,\alpha}(W) = \bar{\mathcal{A}}_\alpha^R \frac{f_{\gamma R}(W) \Gamma_R M_R f_{\pi R}(W)}{M_R^2 - W^2 - iM_R \Gamma_R}, \quad (19)$$

where  $f_{\pi R}$  is the usual Breit-Wigner factor describing the decay of a resonance  $R$  with total width  $\Gamma_R(W)$  and physical mass  $M_R$ . The expressions for  $f_{\gamma R}$ ,  $f_{\pi R}$  and  $\Gamma_R$  are given in Ref. [25]. In the DMT model the electromagnetic form factor  $\bar{\mathcal{A}}_\alpha^R$  describes the bare  $\gamma NR$  vertex. This is a free parameter to be determined from the experimental data.

In Fig. 5 (upper panel) we see that the resonant background in the DMT model (dash-dotted curve) is very important, in particular for  $W > 1450$  MeV where it becomes large and negative. This is in contrast to the prediction based on the K-matrix approximation (dashed curve). The difference comes mainly from the principal value integral contribution in Eq. (18). Such a background will thus require a much stronger resonance contribution in order to describe the results of the recent partial wave analysis of Ref. [28]. Consequently, the dynamical model predicts much larger values for the electromagnetic form factors (or helicity amplitudes  $A_{1/2}$ ) than those obtained with the K-matrix approximation.

In order to estimate the new values for the resonance parameters, we will first fit  $\text{Im } {}_p E_{0+}$  in the photon energy range  $1075 < W < 2300$  MeV only, thereby assuming that  $v_{\gamma\pi}^{R,\alpha} = \sum_{n=1}^4 v_{\gamma\pi}^{R_n,\alpha}$ . The results of our fit are presented in Tables II-IV and Fig. 5. We would like to stress that, since the DMT background is large and negative even at  $W > 1770$  MeV, the best fit requires two new  $S_{11}$  resonances with masses 1800 MeV and 2042 MeV, in addition to the well known resonances  $S_{11}(1535)$  and  $S_{11}(1650)$ . In fact the  $\chi^2$  of the fit improves from 64 to 3.5 by introducing these two additional resonances. This result clearly indicates that, in agreement with our previous findings for pion scattering, our pion photoproduction model calls for a low-lying third  $S_{11}$  resonance which may be one of the missing resonances predicted by quark models [19].

Our next important result concerns the value of the helicity amplitude for the first  $S_{11}(1535)$  resonance. Here we expect to get more reliable information by analyzing the observables (differential cross sections, beam, target and recoil asymmetries) in the full energy range  $1075 < W < 1770$  MeV, similar to the work of Ref. [30]. In other words, we have to perform a new partial wave analysis including the new background description. For this purpose the resonances in the higher partial waves have to be taken into account as well. The details of our fitting procedure are described in Ref. [30]. We only note that our analysis includes experimental data for  $E_\gamma < 1200$  MeV. In the proton channel the corresponding data base contains 14880 data points. We fix the parameters for the third and fourth  $S_{11}$  resonances using the results for  $\text{Im } {}_pE_{0+}$  as described above. Our final results are shown in Fig. 6 and summarized in Table V. In general they are consistent with the earlier results obtained directly from  $\text{Im } {}_pE_{0+}$ .

Our final value for the bare helicity amplitude of the first  $S_{11}(1535)$  resonance is  $A_{1/2}(\text{bare}) = 116 \pm 3 \times 10^{-3} \text{GeV}^{-1/2}$ . In order to obtain the dressed value, we first have to determine the nonresonant background  $\tilde{t}_{\gamma\pi}^{B\alpha}$ , as given by Eq. (16). The result for this background, shown in Fig. 7 (left panel) by the dashed curve, is small near resonance position. The dressed value for the  $A_{1/2}$  can be calculated directly from  $\text{Im } {}_pE_{0+}^{(1/2)}$  using the relation [31]

$$A_{1/2} = -\sqrt{\frac{2\pi M_R \Gamma_R q_R}{k_R m_N \beta_\pi}} \text{Im } {}_pE_{0+}^{(1/2)} C_{\pi N}, \quad (20)$$

where  $q_R$  and  $k_R$  are the pion and photon momentum, respectively, at  $W = M_R = 1528$  MeV and  $C_{\pi N} = -\sqrt{3}$  is an isospin factor. Subtracting the contribution of the other  $S_{11}$  resonances we obtain  $\text{Im } {}_pE_{0+}^{(1/2)} = (3.93 - 0.14) \times 10^{-3}/m_{\pi+}$ , where the last number is the contribution of the nonresonant background  $\tilde{t}_{\gamma\pi}^{B\alpha}$ , and  $A_{1/2}(\text{dressed}) = (72 \pm 2) \times 10^{-3} \text{GeV}^{-1/2}$ . Another separation of the resonance and background contributions can be obtained by use of the K-matrix approximation for pion rescattering. In this case  $\text{Im } {}_pE_{0+}^{(1/2)} = (3.93 - 0.42) \times 10^{-3}/m_{\pi+}$  and the corresponding helicity amplitude  $A_{1/2}(\text{K-matrix}) = (67 \pm 2) \times 10^{-3} \text{GeV}^{-1/2}$ , which is very close to the dressed value obtained above.

As a last step, we extract the bare and dressed values for  $A_{1/2}$  from eta photoproduction. The formalism for this reaction is similar to the pion photoproduction case, the only difference being that in the eta channel it is important to take account of the coupling to the pion channel. The resonant background  $t_{\gamma\eta}^B$  can then be written as

$$t_{\gamma\eta}^B(E) = v_{\gamma\eta}^B + v_{\gamma\eta}^B g_\eta(E) t_{\eta\eta}(E) + v_{\gamma\pi}^B g_\pi(E) t_{\pi\eta}(E), \quad (21)$$

where  $t_{\eta\eta}(E)$  and  $t_{\pi\eta}(E)$  are the full t-matrices describing eta scattering and eta production by pions, respectively, as obtained by solving Eq. (2).

Our results for the resonant background in the  ${}_pE_{0+}$  channel are shown in Fig. 7 (right panel) by the dash-dotted curve. We can see that this background is about 30% of the total amplitude (solid curves), and that it originates mainly from the coupling to the pion channel. Using Eq. (20) (with the eta momentum for  $q_R$ , branching ratio  $\beta_\eta = 0.5$ , and  $C_{\eta N} = -1$ ) we can now extract  $A_{1/2}(\text{bare})$ ,  $A_{1/2}(\text{dressed})$  and  $A_{1/2}(\text{K-matrix})$ . The final results and a comparison with the results obtained for the first  $S_{11}$  resonance in pion photoproduction are given in Table VI. In general the values of the helicity amplitudes derived from the two reactions are consistent within 10%. Note that our bare values are also close to the result obtained in Ref. [34] ( $A_{1/2} = 102 \times 10^{-3} \text{GeV}^{-1/2}$ ) by solving of the coupled Bethe-Salpeter equations. However, our dressed value considerably differs from the results of Ref. [32] where  $A_{1/2}(\text{dressed}) = 118 \times 10^{-3} \text{GeV}^{-1/2}$ . This is mainly due to the different total width  $\Gamma_R$ , which is 191 MeV in Ref. [32] and 95 MeV in our model. For example using Eq. (20), we can easily obtain that  $A_{1/2}(\text{dressed}) \simeq 118 \sqrt{95/191} = 83 \times 10^{-3} \text{GeV}^{-1/2}$  which is close to our result.

The comparison with the results of others groups are given in Table VII. Here we present only the dressed values for the helicity amplitude of the first  $S_{11}$  resonance. Our corresponding background is shown in Fig. 7 (left panel) by the dashed curve which does not contain the pion loop contribution in the electromagnetic vertex (last diagram of Fig. 4). At the resonance position this background is very close to the backgrounds of the Pitt-ANL and GW-Giessen groups [10]. Therefore, we expect that the values for the helicity amplitudes will also be close if the other resonance parameters ( $\Gamma_R$  and  $\beta_\pi$ ) are the same. With this condition a simple recalculation of the Pitt-ANL results yields  $A_{1/2}(\text{dressed}) \simeq 87 \sqrt{0.35/112 \cdot 95/0.40} = 74 \times 10^{-3} \text{GeV}^{-1/2}$ , which is close to our value. In a similar way we obtain  $A_{1/2}(\text{dressed}) \simeq 60 \times 10^{-3} \text{GeV}^{-1/2}$  for the GW-Giessen results. Large differences remain only with the results of the KSU analysis, and this is mainly connected with a larger the background contribution in the KSU model (see Fig. 1 in Ref. [10]).

We thus conclude that the large differences for the helicity amplitude of the  $S_{11}(1535)$  resonance obtained in different analyses, are due to the differences for the total widths and differences in the background description. From our coupled channel analysis of pion scattering and pion photoproduction reactions, we obtain  $\Gamma_R \simeq 100$  MeV. Note

that values close to ours were also obtained within the Pit-ANL and KSU models [10] and in Refs. [27,28]. It seems that in order to clarify the situation for the total width, a new analysis of eta photoproduction is required, especially with the additional background contributions appearing due to the coupling to the pion channel.

#### IV. CONCLUSION

We have performed a self-consistent analysis of pion scattering and pion photoproduction within a coupled channels dynamical model. In the case of pion photoproduction, we obtain background contributions to the imaginary part of the  $S$ - wave multipole which differ considerably from the result based on the K-matrix approximation. Within the dynamical model these background contributions become large and negative in the region of the  $S_{11}(1535)$  resonance. Due to this fact much larger resonance contributions are required in order to explain the results of the recent multipole analyses. For the first  $S_{11}(1535)$  resonance we obtain as values of the bare and dressed electromagnetic helicity amplitudes:  $A_{1/2}(\text{bare}) = (116 \pm 3) \times 10^{-3} \text{GeV}^{-1/2}$  and  $A_{1/2}(\text{dressed}) = (72 \pm 2) \times 10^{-3} \text{GeV}^{-1/2}$ . Similar values can be derived from eta photoproduction if one takes the same total width ( $\Gamma_R = 95 \pm 5 \text{ MeV}$ ) as in pion scattering and pion photoproduction.

At invariant energy  $W \geq 1750 \text{ MeV}$ , our analysis yields considerable strength, which can be described by a third and a fourth  $S_{11}$  resonance with the masses  $1846 \pm 47$  and  $2113 \pm 70 \text{ MeV}$ . Such resonances are also predicted by quark models. However, our coupled channels approach yields large resonance widths of the order of 300 MeV or more, and therefore the energy dependence of the  $S_{11}$  amplitude is not very pronounced at these higher energies. Whether or not these indications for higher  $S_{11}$  strengths will eventually lead to well-established resonances, will strongly depend on future experiments and analyses of final states with uncorrelated two-pion systems,  $\rho$  and  $\omega$  mesons and sequential decays like the  $\rho - \Delta$  process.

#### ACKNOWLEDGMENTS

S.K. and L.T. are grateful to the Physics Department of the NTU for the hospitality extended to them during their visits. This work is supported in part by the National Science Council/ROC under grant NSC 90-2112-M002-032, by the Deutsche Forschungsgemeinschaft (SFB 443), and by a joint project NSC/DFG TAI-113/10/0.

---

\* Permanent address: Laboratory of Theoretical Physics, JINR Dubna, 141980 Moscow region, Russia.

- [1] Particle Data Group, Phys. Rev. D66 (2002) 010001-1.
- [2] R. A. Arndt, I.I. Strakovsky, R.L. Workman, and M.M. Pavan, Phys. Rev. C52 (1995) 2120.
- [3] G. Höhler, F. Kaiser, R. Koch, and E. Pietarinen, *Handbook of Pion-Nucleon Scattering*, [Physics Data No. 12-1 (1979)].
- [4] D. M. Manley and E. M. Saleski, Phys. Rev. D45 (1992) 4002.
- [5] T. Feuster and U. Mosel, Phys. Rev. C58 (1998) 457.
- [6] R. E. Cutkovsky, C. P. Forsyth, R. E. Hendrick, and R. L. Kelly, Phys. Rev. D20 (1979) 2839.
- [7] C. Bennhold and H. Tanabe, Nucl. Phys. A350 (1991) 625.
- [8] M. Batinic, I. Slaus and A. Svarc, Phys. Rev. C51 (1995) 2310.
- [9] T. P. Vrana, S. A. Dytman and T.-S. Lee, Phys. Rep. 328 (2000) 181.
- [10] Bennhold et al. Proc. of NSTAR2001 workshop, Mainz 2001, eds D. Drechsel and L. Tiator (World Scientific, 2001), p.109.
- [11] E. Oset and A. Ramos, Nucl. Phys. A635 (1998) 99
- [12] H. Tanabe and K. Ohta, Phys. Rev. C31 (1985) 1876.
- [13] S. N. Yang, J. Phys. G11 (1985) L205.
- [14] S. Nozawa, B. Blankleider and T.-S. H. Lee, Nucl. Phys. A513 (1990) 459; S. Nozawa and T.-S. Lee, Nucl. Phys. A513 (1990) 511.
- [15] C. T. Hung, S. N. Yang, and T.-S.H. Lee, J. Phys. G20 (1994) 1531; Phys. Rev. C64 (2001) 034309.
- [16] S. S. Kamalov and S. N. Yang, Phys. Rev. Lett. 83 (1999) 4494.
- [17] S. S. Kamalov, S. N. Yang, D. Drechsel, O. Hanstein, and L. Tiator, Phys. Rec. C64 (2001) 032201(R).
- [18] S. S. Kamalov, G.-Y. Chen, S. N. Yang, D. Drechsel, and L. Tiator, Phys. Let. B 522 (2001) 27.
- [19] M. M. Giannini, E. Santopinto, A. Vassallo, Nucl. Phys. A699 (2002) 308.
- [20] B. Saghai and Zhenping Li, nucl-th/0202007.

- [21] M. Cooper and B. Jennings, Nucl. Phys. A500 (1989) 553.
- [22] L. Tiator, C. Bennhold and S. S. Kamalov, Nucl. Phys. A580 (1994) 455.
- [23] B. C. Pearce and B. Jennings. Nucl. Phys. A528 (1991) 655.
- [24] A. I. L'vov, V. A. Petrun'kin and M. Schumacher, Phys. Rev. C55 (1997) 359.
- [25] D. Drechsel, O. Hanstein, S.S. Kamalov, and L. Tiator, Nucl. Phys. A645 (1999) 145.
- [26] R. A. Arndt, I. I. Strakovsky, R. L. Workman, and M. M. Pavan, Phys. Rev. C52 (1995) 2120
- [27] T. Inoue, E. Oset and M.J. Vicente Vacas, Phys. Rev. C65 (2002) 0352004.
- [28] R. A. Arndt, W. J. Briscoe, I. I. Strakovsky, and R. L. Workman, nucl-th/0205067 and private communication.
- [29] T. Sato and T.-S.H. Lee, Phys. Rev. C54 (1996) 2660.
- [30] S. S. Kamalov, D. Drechsel, L. Tiator, and S. N. Yang, Proc. of NSTAR2001 workshop, Mainz 2001, eds D. Drechsel and L. Tiator (World Scientific, 2001), p.197, (s.a.) nucl-th/0106045.
- [31] R. A. Arndt, R. L. Workman, Zh. Li, and L. D. Roper, Phys. Rev. C42 (1990) 1864.
- [32] W. T. Chiang, S. N. Yang, L. Tiator, and D. Drechsel, Nucl.Phys. A700 (2002) 429.
- [33] O. Hanstein, D. Drechsel, and L. Tiator, Nucl. Phys. A632 (1998) 561.
- [34] C. Deutsch-Sauermann, B. Friman and W. Nörenberg. Phys. Lett. B409 (1997) 51.

	$R_1$	$R_2$	$R_3$	$R_4$	
$M_R$ (MeV)	1520(6)	1677(6)	1893(18)	2183(21)	our result
	1542(3)	1689(12)	1822(43)	—	Pitt-ANL
	1528(1)	1649(1)	2000(1)	—	KSU
	1549(7)	1690(11)	—	—	GW-Giessen
	1520-1555	1640-1680	$\sim 2090$	—	PDG2002
$\Gamma_R$ (MeV)	95(10)	195(14)	265(31)	427(26)	our result
	112(19)	202(40)	248(185)	—	Pitt-ANL
	111(9)	108(14)	132(16)	—	KSU
	232(19)	206(13)	—	—	GW-Giessen
	100-200	145-190	—	—	PDG2002
$\Gamma_\pi/\Gamma_R$ (%)	40(7)	75(4)	44(5)	43(2)	our result
	35(5)	74(2)	17(7)	—	Pitt-ANL
	41(3)	32(5)	10(3)	—	KSU
	30(1)	60(7)	—	—	GW-Giessen
	35-55	55-90	—	—	PDG2002
$\Gamma_\eta/\Gamma_R$ (%)	40(7)	11(3)	12(7)	3(6)	our result
	51(5)	6(1)	41(4)	—	Pitt-ANL
	50(4)	5(3)	3(2)	—	KSU
	63(3)	11(1)	—	—	GW-Giessen
	30-55	3-10	—	—	PDG2002

TABLE I.  $S_{11}$  resonance parameters obtained from  $\pi N$  scattering and  $\pi N \rightarrow \eta N$ , and comparison with the results of the Pitt-ANL, KSU and GW-Giessen groups taken from Ref. [10]. Recent PDG values from Ref. [1].

Parameters	$\beta_\pi = \Gamma_\pi/\Gamma_R$	$M_R$	$\Gamma_R$	$A_{1/2}$ (bare)
$R_1$	0.40	$1523 \pm 3$	$97 \pm 7$	$110 \pm 7$
$R_2$	0.75	$1689 \pm 3$	$164 \pm 8$	$142 \pm 6$

TABLE II. Estimation of the  $S_{11}$  resonance parameters obtained by fitting  $\text{Im } {}_pE_{0+}$  in the energy range  $145 \text{ MeV} < E_\gamma < 1200 \text{ MeV}$  ( $1075 \text{ MeV} < W < 1900 \text{ MeV}$ ), with only two  $S_{11}$  resonances. Helicity amplitudes  $A_{1/2}$  are given in units  $10^{-3} \text{ GeV}^{-1/2}$ .

Parameters	$\beta_\pi = \Gamma_\pi/\Gamma_R$	$M_R$	$\Gamma_R$	$A_{1/2}$ (bare)
$R_1$	0.40	$1523 \pm 3$	$97 \pm 7$	$110 \pm 7$
$R_2$	0.75	$1689 \pm 3$	$160 \pm 11$	$119 \pm 5$
$R_3$	0.44	$1962 \pm 10$	$503 \pm 80$	$131 \pm 7$

TABLE III. Estimation of  $S_{11}$  resonance parameters obtained by fitting  $\text{Im } {}_pE_{0+}$  in the energy range  $145 \text{ MeV} < E_\gamma < 2000 \text{ MeV}$  ( $1075 \text{ MeV} < W < 2300 \text{ MeV}$ ), with three  $S_{11}$  resonances ( $\chi^2/95 = 4.7$ ). The parameters for the first  $S_{11}$  resonance were fixed according to Table I. Helicity amplitudes  $A_{1/2}$  are given in units  $10^{-3} \text{ GeV}^{-1/2}$ .

Parameters	$\beta_\pi = \Gamma_\pi/\Gamma_R$	$M_R$	$\Gamma_R$	$A_{1/2}(\text{bare})$
$R_1$	0.40	$1523 \pm 3$ (1524)	$97 \pm 7$	$110 \pm 7$
$R_2$	0.75	$1677 \pm 3$ (1688)	$116 \pm 8$	$83 \pm 6$
$R_3$	0.44	$1799 \pm 9$ (1861)	$314 \pm 11$	$129 \pm 9$
$R_4$	0.43	$2042 \pm 16$ (2008)	$288 \pm 29$	$61 \pm 8$

TABLE IV. Estimation of the  $S_{11}$  resonance parameters obtained by fitting  $\text{Im } p E_{0+}$  in the energy range  $145 \text{ MeV} < E_\gamma < 2000 \text{ MeV}$  ( $1075 \text{ MeV} < W < 2300 \text{ MeV}$ ), with four  $S_{11}$  resonances ( $\chi^2/95 = 3.5$ ). The parameters for the first  $S_{11}$  resonance were fixed according to Table I. In brackets: quark model predictions of Ref. [19] for the masses  $M_R$ . Helicity amplitudes  $A_{1/2}$  are given in units  $10^{-3} \text{ GeV}^{-1/2}$ .

Parameters	$M_R$	$\Gamma_R$	$A_{1/2}(\text{bare})$
$R_1$	$1528 \pm 1$	$95 \pm 5$	$116 \pm 3$
$R_2$	$1684 \pm 1$	$112 \pm 7$	$72 \pm 2$

TABLE V. Our final results for the resonance parameters of the first two  $S_{11}$  resonances obtained by fitting the observables in the energy range  $145 \text{ MeV} < E_\gamma < 1200 \text{ MeV}$  ( $1075 \text{ MeV} < W < 1770 \text{ MeV}$ ). The parameters for the third and fourth  $S_{11}$  resonances were fixed with the values from Table IV. The branching ratios are  $\beta_\pi=0.4$  and  $0.75$  for  $R_1$  and  $R_2$ , respectively.

$A_{1/2}$	$(\gamma, \pi)$	$(\gamma, \eta)$
$A_{1/2}(\text{bare})$	$116 \pm 3$ (6.1)	$108 \pm 4$ (17.8)
$A_{1/2}(\text{dressed})$	$72 \pm 2$ (3.8)	$81 \pm 3$ (13.5)
$A_{1/2}(\text{K-matrix})$	$67 \pm 2$ (3.5)	$83 \pm 3$ (13.8)

TABLE VI.  $A_{1/2}(\text{bare})$ ,  $A_{1/2}(\text{dressed})$  and  $A_{1/2}(\text{K-matrix})$  helicity amplitudes (in units  $10^{-3} \text{ GeV}^{-1/2}$ ) for the  $S_{11}(1535)$  resonance obtained in pion and eta photoproduction using the coupled channel dynamical model (see text). The values correspond to  $M_R = 1528 \text{ MeV}$ ,  $\Gamma_R = 95 \text{ MeV}$ ,  $\beta_\pi = 0.4$ , and  $\beta_\eta = 0.5$ . In the brackets we give the imaginary part of the corresponding  $E_{0+}$  multipoles at the resonance position in units of  $10^{-3}/m_{\pi^+}$ .

Ref.	$\beta_\pi = \frac{\Gamma_\pi}{\Gamma_R}$	$\Gamma_R(\text{MeV})$	$A_{1/2}(\text{dressed})$
our	$0.40 \pm 0.07$	$95 \pm 5$	$72 \pm 2$
Pitt-ANL	$0.35 \pm 0.05$	$112 \pm 19$	$87 \pm 3$
KSU	$0.41 \pm 0.03$	$111 \pm 9$	$42 \pm 6$
GW-Giessen	$0.30 \pm 0.01$	$232 \pm 19$	$106 \pm 5$
PDG2002	$0.35 - 0.55$	$100 - 200$	$90 \pm 30$

TABLE VII. Resonance parameters and helicity amplitudes  $A_{1/2}(\text{dressed})$  (in units  $10^{-3} \text{ GeV}^{-1/2}$ ) for the  $S_{11}(1535)$  resonance and comparison with the results of the Pitt-ANL, KSU and GW-Giessen groups taken from Ref. [10]. Recent PDG values from Ref. [1].

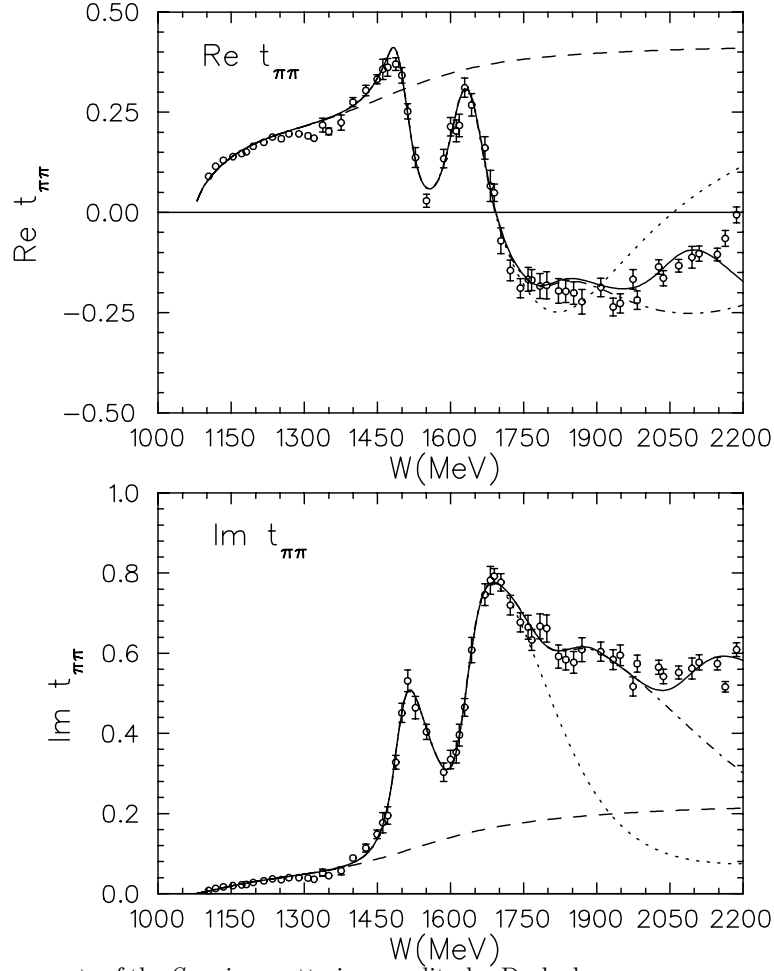


FIG. 1. Real and imaginary parts of the  $S_{11}$  pion scattering amplitude. Dashed curves: nonresonant background contribution  $\tilde{t}_{\pi\pi}^B$ . Dotted, dash-dotted, and solid curves: total  $t_{\pi\pi}$  amplitude obtained after the best fit with two, three, and four  $S_{11}$  resonances, respectively. Data points: results of the single energy analysis from Ref. [26].

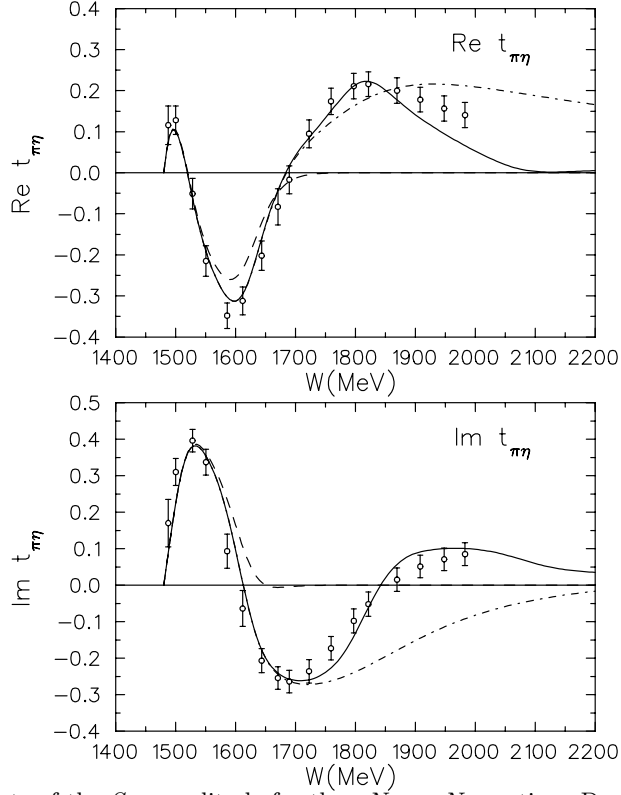


FIG. 2. Real and imaginary parts of the  $S_{11}$  amplitude for the  $\pi N \rightarrow \eta N$  reaction. Dashed curves, dash-dotted, and solid curves are the results obtained with  $R_1$ ,  $R_1 + R_2$ , and  $R_1 + R_2 + R_3$  contributions, respectively. We did not find evidence for a fourth  $S_{11}$  in this reaction. Data points: results of the partial wave analysis from Ref. [9].

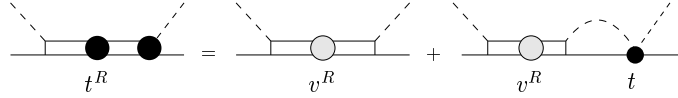


FIG. 3. Graphical representation of the resonance contribution to pion scattering as determined by Eq. (8). The grey circle in the resonance propagators denotes the presence of the width associated with the  $\pi\pi N$  contribution, the black circle corresponds to the propagators with total width and physical mass.

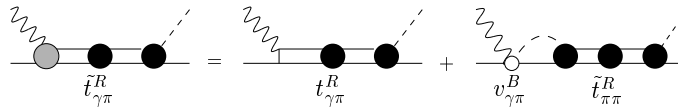


FIG. 4. Graphical representation of the resonances with dressed and bare electromagnetic vertices.

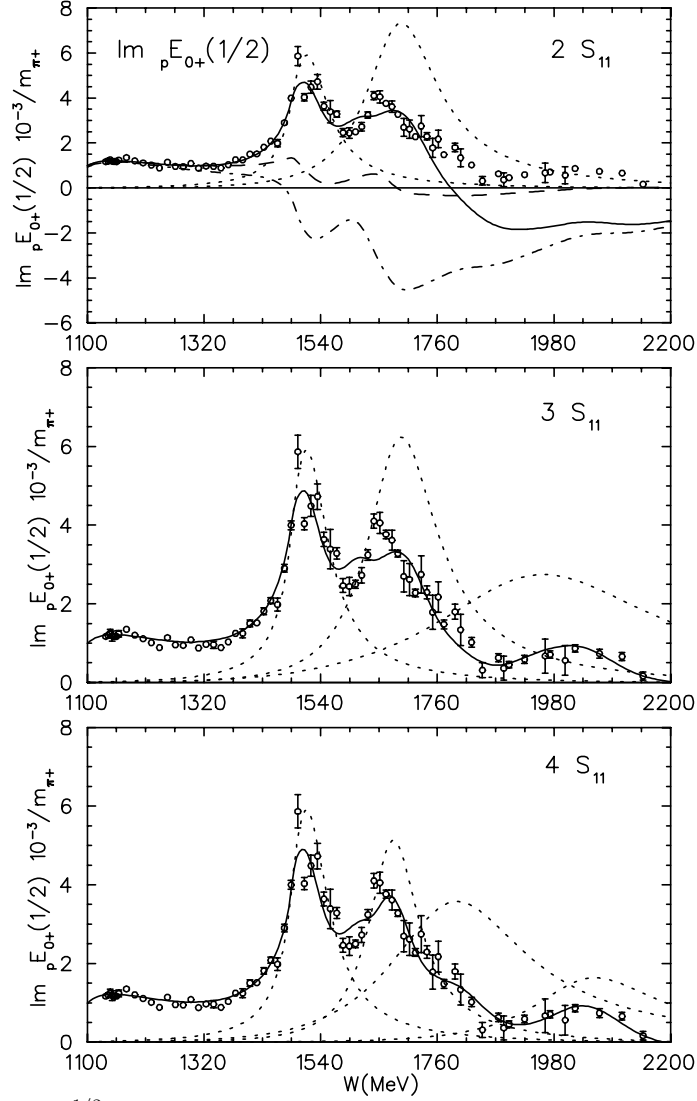


FIG. 5. Imaginary parts of the  ${}_p E_{0+}^{1/2}$  multipoles. Dashed and dash-dotted curves in the upper panel: background contributions obtained using K-matrix approximation and DMT model, respectively. Solid curves in the upper, middle and lower panels: total multipole with two, three, and four  $S_{11}$  resonances, respectively. The individual contributions from each resonance (with bare electromagnetic vertex) are shown by the dotted curves. The corresponding resonance parameters are given in Tables II-IV. Data points: results of the single energy multipole analysis from Ref. [28].

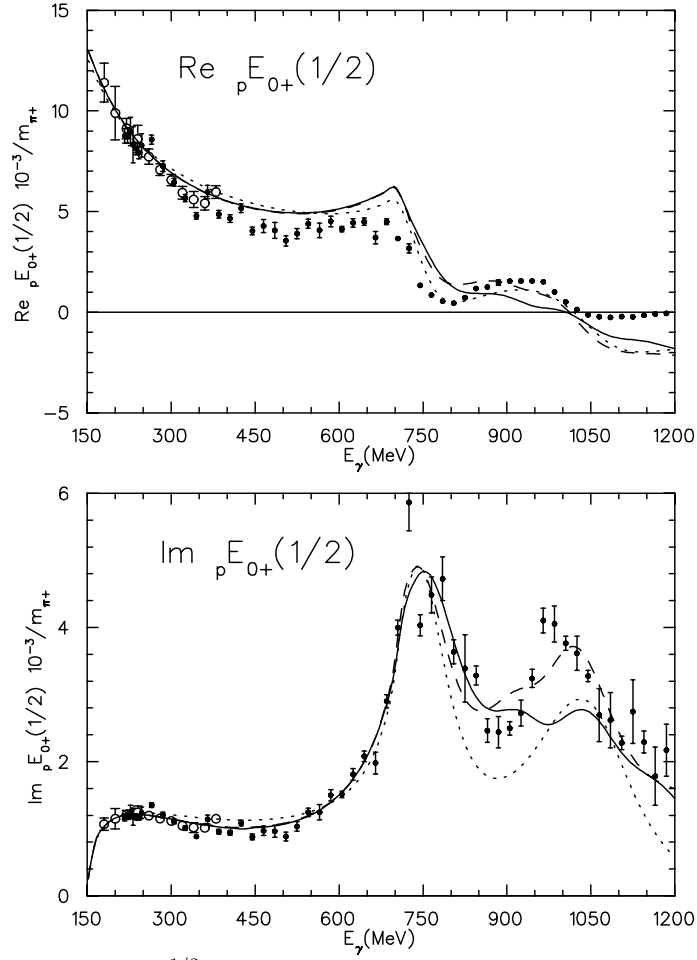


FIG. 6. Real and imaginary parts of the  $p E_{0+}^{1/2}$  multipole. Dashed and solid curves: results obtained by fitting  $\text{Im } p E_{0+}^{1/2}$  (see Table IV) and the observables (see Table V), respectively. Dotted curve: result of MAID2000 [25]. Data points: results of the single-energy multipole analysis of Ref. [33] (○) and Ref. [28] (●).

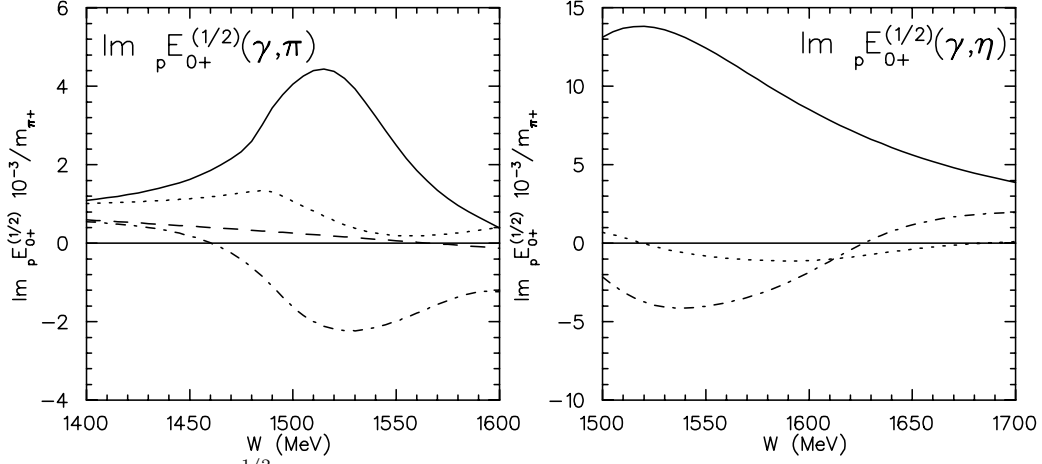


FIG. 7. Imaginary parts of the  ${}_p E_{0+}^{1/2}$  multipoles for pion (left figure) and eta (right figure) photoproduction on the proton. Dash-dotted and dashed curves are resonant,  $t^B$  (Eqs.(13-15)), and nonresonant,  $\tilde{t}^B$  (Eq.(16)), backgrounds, respectively. In the case of eta photoproduction, the main contribution to the resonant background comes from the coupling to the  $\pi\eta$  channel, the contribution  $\tilde{t}^B$  of the nonresonant background vanishes. Dotted curves: background according to the K-matrix approximation. Solid curves: total result including contributions of  $S_{11}(1535)$  resonance and background, taken from Ref [32].